Power Engineering and Engineering Thermophysics
https://www.acadlore.com/journals/PEET

Enhancing the Sustainability of PVT Systems Through Optimized PCM Selection and Container Configuration: A CFD Approach

Royb Fathur Rizal*, Misbahul Munir

Department of Power Plant Engineering Technology, State University of Malang, 65145 Malang, Indonesia

* Correspondence: Royb Fathur Rizal (fatkhurrizal.fv@um.ac.id)

Received: 11-14-2024 **Revised:** 12-17-2024 **Accepted:** 12-25-2024

Citation: R. F. Rizal and M. Munir, "Enhancing the sustainability of PVT systems through optimized PCM selection and container configuration: A CFD approach," *Power Eng. Eng. Thermophys.*, vol. 3, no. 4, pp. 266–278, 2024. https://doi.org/10.56578/peet030404.

Abstract: The thermal performance and energy efficiency of Photovoltaic Thermal (PVT) systems were investigated through the integration of Phase Change Materials (PCMs) combined with distinct container configurations. Two types of PCMs—paraffin wax, an organic material, and Polyethylene Glycol 1000 (PEG-1000), a polymer-based alternative—were embedded within two container designs: a plain container and a baffled container. To evaluate the impact of PCM selection and container geometry on system performance, a series of numerical simulations were conducted using Computational Fluid Dynamics (CFD) in ANSYS Fluent under varying solar irradiance levels of 300, 600, 900, and 1200 $\mathrm{W/m^2}$. The results revealed that PCM integration significantly mitigates the operating temperature of PV cells, contributing to enhanced thermal stability and electrical conversion efficiency. At the highest irradiance of 1200 $\mathrm{W/m^2}$, the plain paraffin configuration attained a minimum cell temperature of 27.4°C and achieved the highest electrical efficiency of 11.7%. Conversely, the baffled PEG-1000 configuration exhibited a slightly higher peak temperature of 28.1°C with a corresponding efficiency of 11.18%. Although the baffled container promoted improved internal heat distribution, the plain configuration demonstrated superior overall thermal regulation. These findings underscore the critical influence of PCM thermal properties and container geometry on the operational sustainability of PVT systems. This study provides new insights into PCM-container coupling strategies, offering a valuable framework for the development of high-efficiency, sustainable solar energy systems.

Keywords: Computational Fluid Dynamics (CFD); Photovoltaic Thermal (PVT); Phase Change Material (PCM); Thermal management; Solar energy sustainability

1 Introduction

The development of renewable energy technologies, especially solar energy, continues to be a key focus in facing the challenges of sustainable global energy needs [1–3]. One of the crucial innovations in this field is the PVT system, which combines the simultaneous production of electricity and heat in a single unit [4–6]. Although PVT systems offer many advantages, such as increased energy density and total efficiency, one of the main obstacles is the rise in excess temperature in the photovoltaic module, which can lower electrical efficiency and accelerate material degradation [7–9]. To overcome this problem, the integration of PCM is an innovative approach that is increasingly popular [10–12]. PCM serves as a latent energy storer that can absorb and release heat during the phase change process, thus helping to keep the temperature of the Photovoltaic (PV) module within the optimal range [13–15]. The selection of the PCM type and the storage container's design are two crucial aspects that significantly affect the system's thermal performance. Paraffin wax (organic PCM) and PEG-1000 (polymeric PCM) are two promising types of PCMs because they have a suitable melting point for PV applications and stable thermal properties [16–18].

The shape of the PCM container also plays a vital role in improving heat transfer efficiency [19, 20]. Plain and baffled container models offer different heat flow and distribution characteristics, which have the potential to affect system performance significantly [8, 21, 22]. Therefore, numerical simulation-based research, such as CFD, has become very relevant to systematically evaluate and compare these various configurations without requiring the high cost of physical experiments [15, 23, 24]. Table 1 summarizes recent studies showing multiple PCM innovations for PV cooling applications. These studies highlight the importance of container design, material selection, and the utilization of advanced simulation methods to achieve improved system performance.

Table 1. Test results of classification

Reference	Novelty	PCM Used	Key Findings
[25]	Experimental study with seasonal outdoor tests and machine learning (ANN) modeling for PV cooling using finned and porous PCM containers.	Paraffin	The porous container achieved $3.40°C$ cooling and a 3.56% efficiency increase in winter. The finned container achieved $3.42°C$ cooling and a 6.58% efficiency increase in summer. ANN models predicted PV temperature and power with $R^2 = 0.98 - 0.99$.
[26]	CFD simulation of PCM containers (horizontal and cylindrical) with and without. solid/hollow fins for solar dryers	Paraffin RT58	Horizontal rectangular containers had the fastest melting and solidification. Solid fins reduced melting/solidification time better than hollow fins, but hollow fins were lighter and more economical.
[27]	Numerical study of fin shapes and nanoparticle-enhanced PCM in a PVT system.	Paraffin + nano-SiC, nano- Al_2O_3	10 T -shaped fins reduced PV temperature by 5.03% compared to 6 fins. Nanoparticle addition improved the PCM melting fraction by 2.13%.
[28]	Finite element simulation of PV modules integrated with Docosane PCM under a hot climate.	Docosane $C_{22}H_{46}$	Cell temperature reduced by 78.4% at peak solar flux, overall 31.1% reduction. PV efficiency increased by 10.88%, voltage by 6.1%, and daily power output by 2.1%.
[29]	CFD-based optimization of PV cooling using composite PCM-metal matrices.	RT25 (optimal), $CaCl_2 \cdot 6H_2O$, paraffin, SP29, n-octadecane + aluminum, copper, steel matrices	RT25 sphere showed the best compatibility. High-conductivity metal matrices enhanced thermal distribution. Plastics were less effective.

Based on the existing research, this study focuses on CFD simulation analysis to compare the thermal performance between two PCM container designs, namely plain container and baffled container, using two types of PCMs, namely paraffin and PEG-1000. The main objective of this study is to evaluate the influence of container design and PCM on PV cell efficiency in PVT-PCM systems. CFD simulations were used in this study to describe the temperature distribution in each container design and PCM type. The results of this analysis are expected to provide more in-depth insights into the optimal material selection and container design. Thus, this research is expected to be a scientific basis for developing a more effective and efficient PVT-PCM system.

2 Methodology

This research was conducted using a numerical simulation approach with CFD to evaluate the thermal characteristics of a PVT system integrated with PCM as a passive cooling medium. The simulations were performed using ANSYS Fluent, employing a transient analysis to capture the dynamic thermal behavior over time. Two types of PCM, namely paraffin and PEG-1000, were selected based on their favorable thermophysical properties, including appropriate melting points, high latent heat capacities, and chemical stability, making them well-suited for PV module cooling applications. The physical model was subjected to constant heat flux values of 300 W/m², 600 W/m², 900 W/m², and 1200 W/m², uniformly applied to the top surface of the photovoltaic layer to simulate varying solar irradiance conditions. The computational domain was configured with convective boundary conditions at the outer surfaces, assuming a convective heat transfer coefficient of 8 W/m²·K and an ambient temperature of 33°C. The energy equation was activated, and the flow was modeled using the realizable $k - \varepsilon$ turbulence model to accurately capture heat transfer and fluid behavior within the PCM domain. The simulated system consists of two primary layers: the top is the PV module that receives and absorbs solar heat, and the bottom is the PCM container, functioning as a thermal buffer via latent heat storage. Two container designs, plain and baffled containers, were developed to examine the influence of geometric modifications on thermal performance. Figure 1 shows the illustration of a PVT system. The geometrical dimensions of both container types are detailed in Table 2 and visually represented in Figure 2.

SolidWorks software was used for the two-dimensional modeling of photovoltaic cell systems and PCM containers. This enables a high accuracy level and detailed depiction of geometry for advanced numerical analysis needs. This design process was carried out using a laptop equipped with an AMD Ryzen 5 7520U processor with Radeon graphics, with a speed of 2.80 GHz, aiming to provide optimal support in the modeling and rendering process. After the geometric design stage, thermal performance simulation and phase change processes on the PCM were carried out using ANSYS Fluent software versions 18.2 and 22 to accurately capture the melting and freezing phenomena in the

PCM container. 12 mm mesh elements were used uniformly across the simulation domain to optimize the balance between accuracy and computational efficiency. With this configuration, 27,404 and 45,399 elements were generated for the plain container model, while 29,905 and 53,054 elements for the baffled container model. All simulation parameters, including the thermophysical properties of the material and the boundary conditions, are fully detailed in Table 3.

Figure 1. Illustration of a PVT system

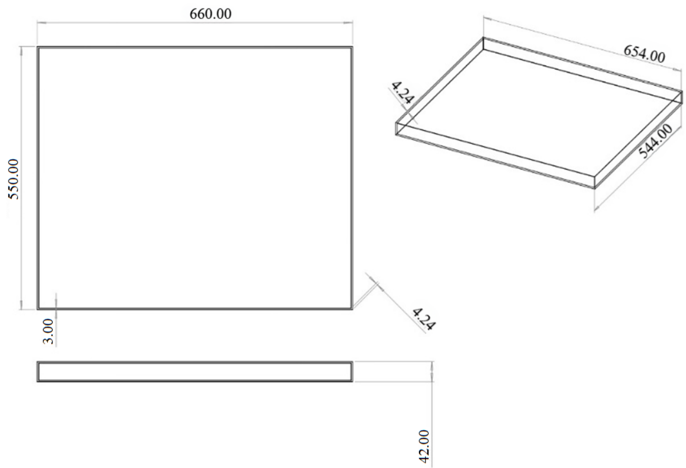

(a)

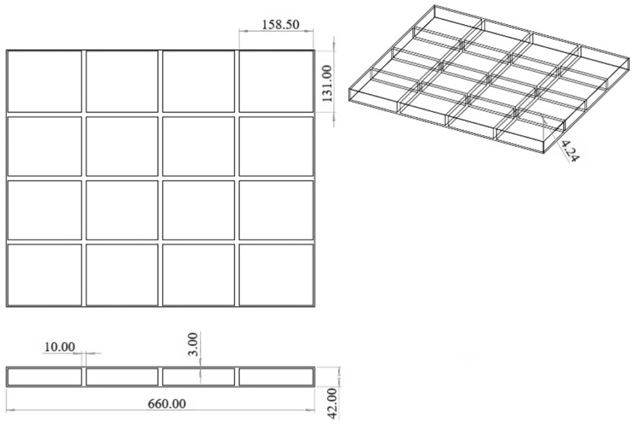

(b)

Figure 2. Dimensions of the PCM container (a) plain, (b) baffled

Table 2. Test results of classification

Specification	Detail
Material	Aluminum
Total size $(W \times W \times H)$	$660 \times 550 \times 42$ mm

Table 3. Thermophysical properties of various materials [16, 30, 31]

Material	Density (kg/ m^3)	Specific Heat (J/kg•K)	Thermal Conductivity (W/mK)	Viscosity $(\mathrm{kg/m^{-5}})$	Pure Solvent Melting Heat (J/kg)	Solidus Temperature (K)	Liquidus Temperature (K)
PV cell	2330	667	130	-	-	-	-
Aluminum	2719	871	202.4	-	-	-	-
Paraffin	@800 @790	2150	0.2	0.01	240800	313.6	317.7
PEG-1000	@1250 @1100	2400	0.31	0.043	254000	307.15	310.15

3 Theoretical Framework and Governing Equations

Numerical studies on PVT-PCM systems have been carried out using the energy conservation approach, with the temperature distribution and heat transfer process modeled using the following energy equations [32, 33]:

$$\frac{\partial}{\partial t}\left(\rho_h\right)+\nabla \times\left(\rho_{uh}\right)=\nabla \times(k \nabla T) \tag{1}$$

where, ρ is the density $\left(\mathrm{kg/m^3}\right)$, h is the specific enthalpy $(\mathrm{J/kg})$, u is the velocity $(\mathrm{m/s})$, k is the thermal conductivity $(\mathrm{W/m \cdot K})$, T is the temperature (K), t is the time (s), and ∇ is the divergence operator.

In systems involving PCMs, the enthalpy model accumulates total energy, including sensible and latent energy during phase transitions. Total enthalpy can be written as follows [34, 35]:

$$h=C_p\left(T-T_{ref}\right)+\Delta H_f \times f_L \tag{2}$$

where, C_p is the specific heat capacity $(\mathrm{J/kg \cdot K})$, T_{ref} is the reference temperature $(25^{\circ}\mathrm{C})$, ΔH_f is the latent heat of fusion $(\mathrm{J/kg})$, and f is the liquid fraction (0 to 1).

The heat conduction process in PV and PCM follows Fourier's law [20]:

$$q=-k \times \nabla T \tag{3}$$

where, q is the heat flux $\left(\mathrm{W/m^2}\right)$.

To evaluate the thermal performance of the collector system, a thermal efficiency formula was used based on the rise in PCM temperature [23]:

$$q=h_c \times A \times\left(T_s-T_{\infty}\right) \tag{4}$$

where, h_c is the convective heat transfer coefficient $\left(\mathrm{W/m^2 \cdot K}\right)$, A is the surface area $\left(\mathrm{m^2}\right)$, T_s is the surface temperature $({}^{\circ}\mathrm{C})$, and T_{∞} is the ambient temperature $({}^{\circ}\mathrm{C})$.

To evaluate the thermal performance of the collector system, a thermal efficiency formula based on the increase in PCM temperature was used [35]:

$$\eta_{\text{thermal}}=\frac{I_{\text{rad}} \times A}{m \times C_p \times \Delta T} \tag{5}$$

where, η_{thermal} is the thermal efficiency, I_{rad} is the incident solar radiation $\left(\mathrm{W/m^2}\right)$, m is the mass of PCM (kg), and ΔT is the temperature difference $({}^{\circ}\mathrm{C})$.

In addition to assessing the effectiveness of PCM in lowering the temperature of PV cells, the following PV efficiency formula was used [19]:

$$\eta_{pv}=\eta_{\text{ref}}\left[1-\beta_{\text{ref}}\left(T_c-T_{\text{ref}}\right)\right] \tag{6}$$

where, η_{pv} is the electrical efficiency of the PV module, η_{ref} is the reference efficiency at standard test conditions (0.14), β_{ref} is the temperature coefficient of efficiency $(0.00392/^{\circ}\text{C})$, and T_c is the PV cell temperature $(^{\circ}\text{C})$.

All results presented in this study were derived from transient CFD simulations based on the equations above.

4 Results

The PVT system performance was evaluated through a numerical simulation approach with the help of ANSYS Fluent software, using the solidification & melting module to represent the phase change process in PCM. The use of PCM as a storage medium and heat transfer is considered to significantly contribute to optimizing the thermal efficiency of solar collectors. Therefore, numerical simulations were carried out to assess the impact of PCM integration on overall system performance. The CFD method was used comprehensively to model the process of energy transfer, PCM liquefaction dynamics, and heat exchange efficiency. All simulation stages were arranged under transient conditions and executed using ANSYS Fluent software version R18.2 student edition to obtain a comprehensive picture of the thermal behavior that develops in PVT systems.

4.1 Visual Evaluation of PCM Temperature Distribution

Figure 3 shows a visualization of the contour of temperature distribution in PCM using ANSYS R18.2 numerical simulation. Each sub-image represents the thermal conditions of four different PCM configurations: plain paraffin, paraffin insulated, plain PEG-1000, and PEG-1000 insulated. The blue color indicates a lower temperature area (close to 299.998 K), while the gradient to red indicates an increase in temperature to about 300.048 K. In subgraph (a) of Figure 3, the temperature distribution on plain paraffin shows a relatively uniform heat distribution, with several small hotspots evenly distributed. This demonstrates paraffin's thermal conductivity ability to conduct heat efficiently, even without additional structures. Meanwhile, subgraph (b) of Figure 3 shows paraffin with an internal baffle. The temperature contour shows the presence of heat concentration in a particular area that is more localized. The baffle structure restricts heat flow laterally, creating small zones with higher temperatures. This resistance causes heat to accumulate around the baffle, leading to slower and more gradual melting. Subgraph (c) of Figure 3 shows the temperature visualization for plain PEG-1000. The heat dispersion pattern is generally similar to plain paraffin, but with a slightly higher hotspot intensity. This reflects the characteristics of PEG-1000, which has a somewhat wider solidus and liquidus temperature than paraffin. Therefore, the phase change process occurs over a wider temperature range.

In subgraph (d) of Figure 3, the PEG-1000 with baffle shows a temperature distribution pattern almost identical to the partitioned paraffin configuration (subgraph (b) of Figure 3). Hotspots are localized in specific areas affected by the presence of partitions. This phenomenon occurs because paraffin and PEG-1000 have relatively low thermal conductivity characteristics. Hence, the baffle effect on heat transfer resistance is dominant compared to the material's properties. In other words, the heat distribution pattern is influenced more by the structure's geometry (the presence of baffles) than by the variation in the properties of PCM. The similarity of temperature distribution patterns in paraffin baffled and PEG-1000 baffled can be explained scientifically based on the principle of heat conduction resistance. The addition of baffles leads to the dominance of geometric-based thermal resistance, which inhibits the diffusion of heat throughout the volume of the material. Since these two materials both have low conductivity, the structure of the baffle is a major determining factor in heat distribution, resulting in similar temperature contour patterns despite different PCMs.

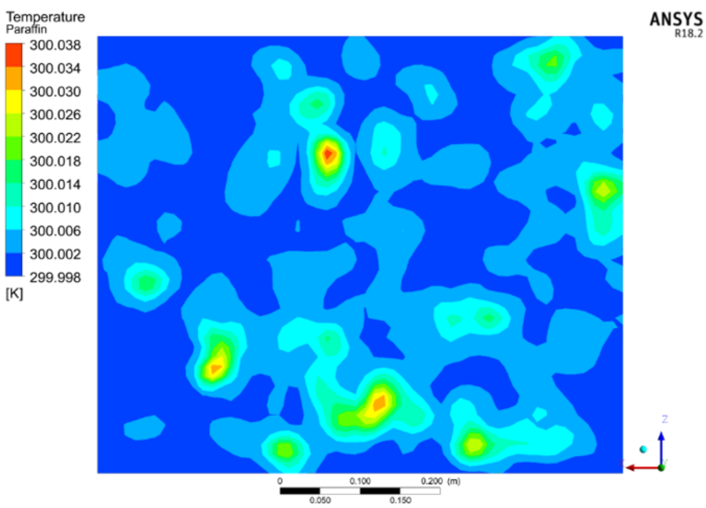

(a)

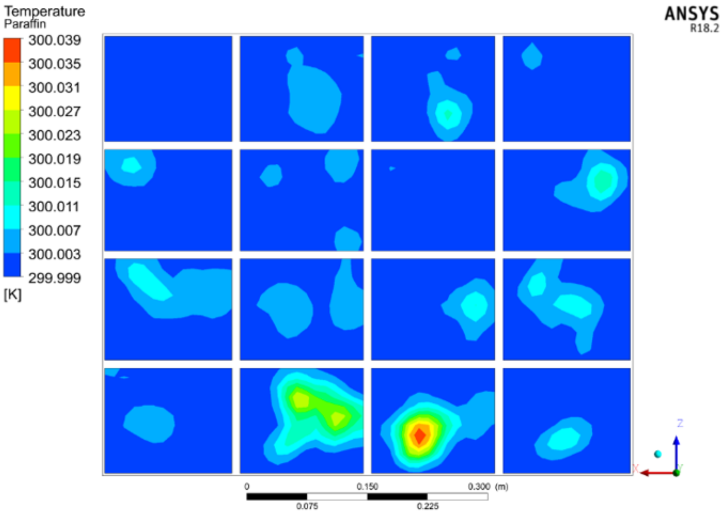

(b)

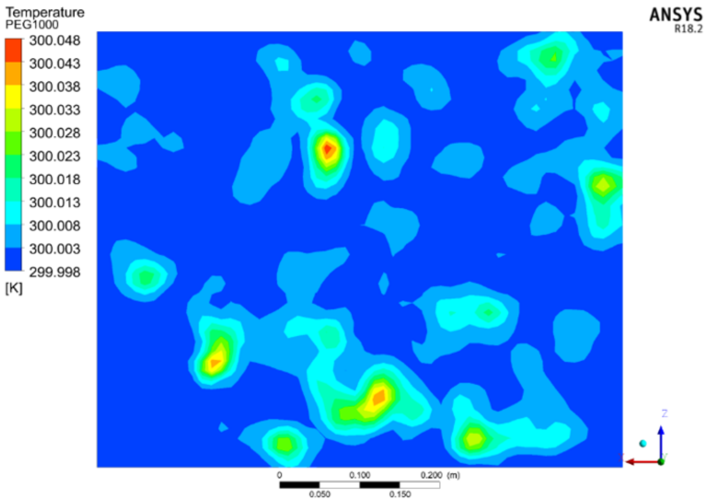

(c)

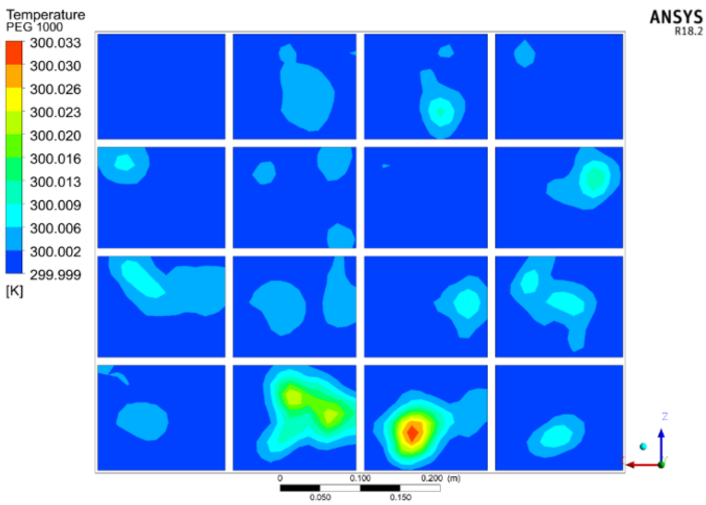

(d)

Figure 3. Contour visualization of PCM: (a) plain paraffin, (b) baffled paraffin, (c) plain PEG-1000, (d) baffled PEG-1000

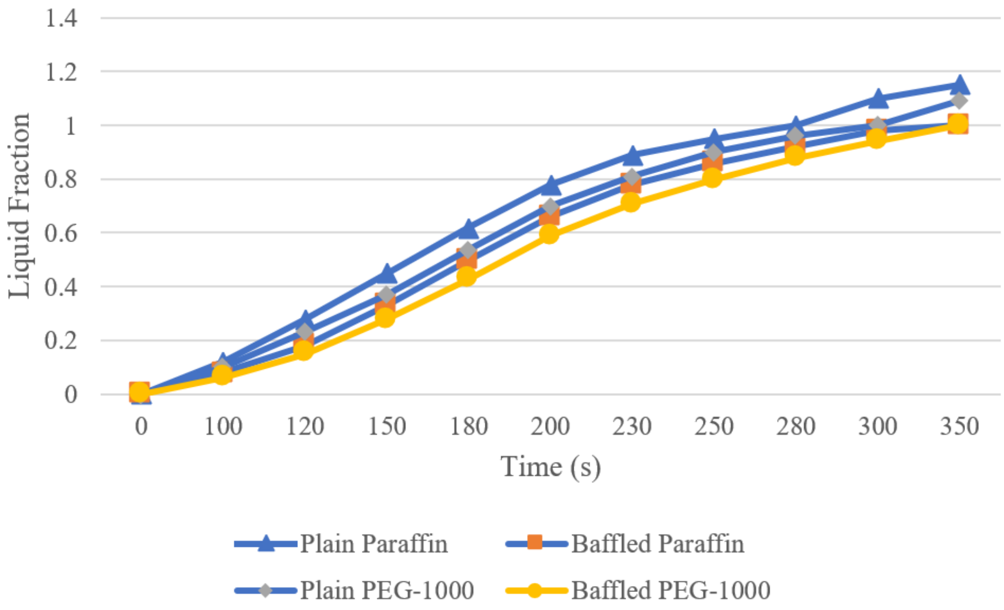

Figure 4. Melting fraction evaluation of PCM

To better understand the PVT-PCM system's dynamic thermal response, each PCM's melting fraction was monitored during a transient CFD simulation under 1200 W/m² irradiance. Figure 4 summarizes the evolution of the liquid fraction for four different configurations. The plain container design allows faster heat transfer, enabling earlier completion of phase change, especially in paraffin. In contrast, baffled containers introduce thermal resistance that delays melting but may promote localized temperature stability. PEG-1000, due to its higher specific heat and broader melting range, requires more time to achieve complete phase transition, which is evident in both container designs.

4.2 Influence of PCM and Design on PV Cell Temperature Distribution

Figure 5 shows a visualization of the contours of the temperature distribution of PV cells using four variations of heat storage media: plain paraffin, paraffin with baffle, plain PEG-1000, and PEG-1000 with baffle. Subgraph (a) of Figure 5 shows the temperature distribution in plain paraffin, with a broader distribution of low temperatures (blue-green zones), indicating a reasonably good cooling ability but with uneven heat distribution. Meanwhile, in subgraph (b) of Figure 5 of the baffled paraffin, the low-temperature distribution is more focused and concentrated in a specific area, showing that baffles can improve heat transfer efficiency by accelerating the release of thermal energy from PCM. Subgraph (c) of Figure 5 shows that plain PEG-1000 has a temperature distribution similar to plain paraffin, but with a slightly more uniform temperature gradient. As for subgraph (d) of Figure 5, the baffled PEG-1000 shows the most concentrated and efficient temperature distribution, with a wider low-temperature area than the baffle-free configuration, proving that combining PEG-1000 material and baffle design synergistically improves the PV cell cooling performance.

From the overall visualization, it can be seen that baffles play an essential role in improving heat distribution in PV cells, both for paraffin and PEG-1000. The presence of baffles creates a more directed heat flow path, accelerates the internal convection process, and improves temperature homogeneity across the solar cell's surface. This visualization also confirms that the temperature contour patterns between all models appear similar due to PCM's basic characteristics of absorbing and storing latent heat that keep surface temperatures within a narrow range. However, slight differences in the concentration and spread of low-temperature zones are essential indicators of the effectiveness of each design. These results are relevant in developing more efficient and sustainable solar energy systems in the future.

4.3 Effect of PCM Container Design on PV Cell Temperature Distribution and Efficiency

Figure 6 shows the comparison of temperature distribution in PV cells equipped with PCM using two types of container models, namely plain and baffled, and two kinds of PCMs, namely paraffin and PEG-1000, against variations in light intensity (300, 600, 900, and 1200 W/m²). In general, the increase in radiation intensity leads to a rise in the surface temperature of the PV cell in all configurations tested. At an intensity of 300 W/m², the highest temperature was achieved by the baffled PEG-1000 configuration of 26.4℃, while the lowest temperature was recorded in plain paraffin at 26.2°C. When the intensity increased to 1200 W/m², a maximum temperature of 28.1°C was indicated by the baffled PEG-1000, while plain paraffin remained at the lowest temperature of 27.4°C.

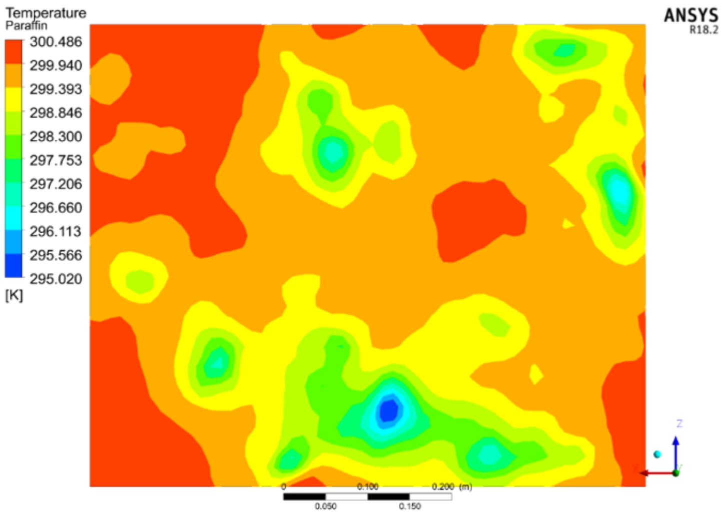

(a)

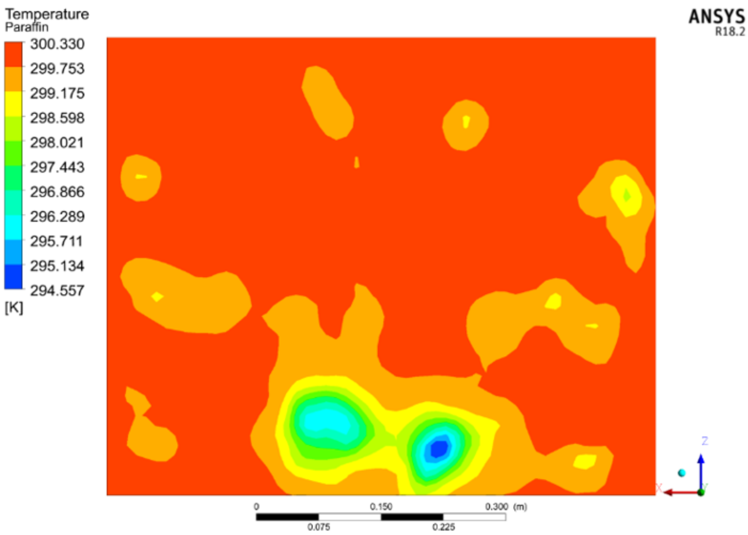

(b)

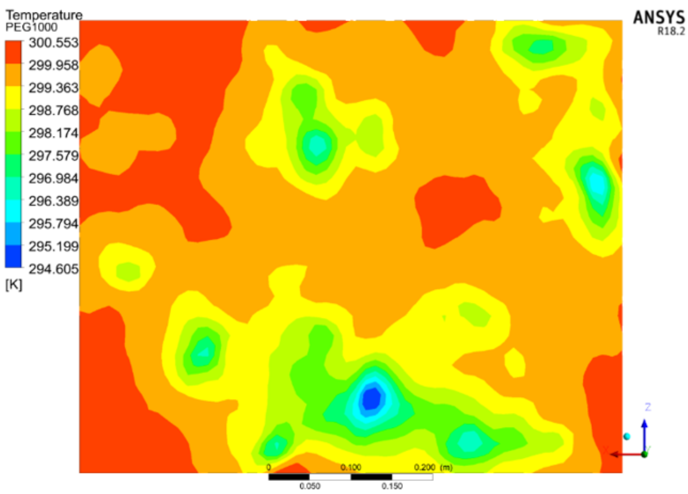

(c)

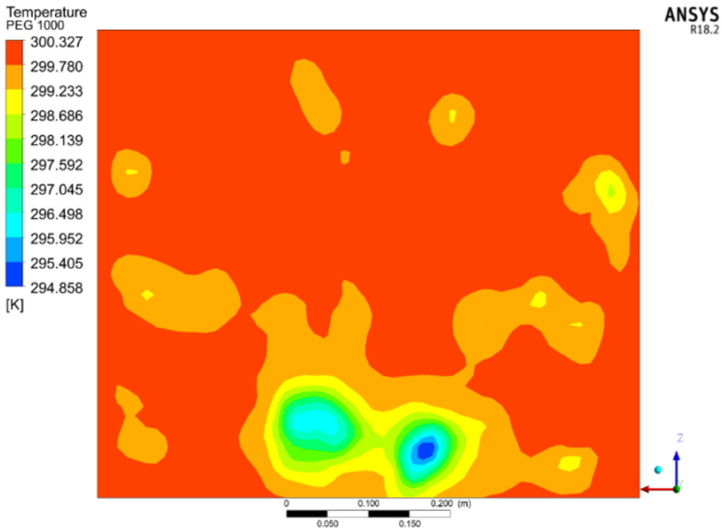

(d)

Figure 5. Contour visualization of PV cell: (a) plain paraffin, (b) baffled paraffin, (c) plain PEG-1000, (d) baffled PEG-1000

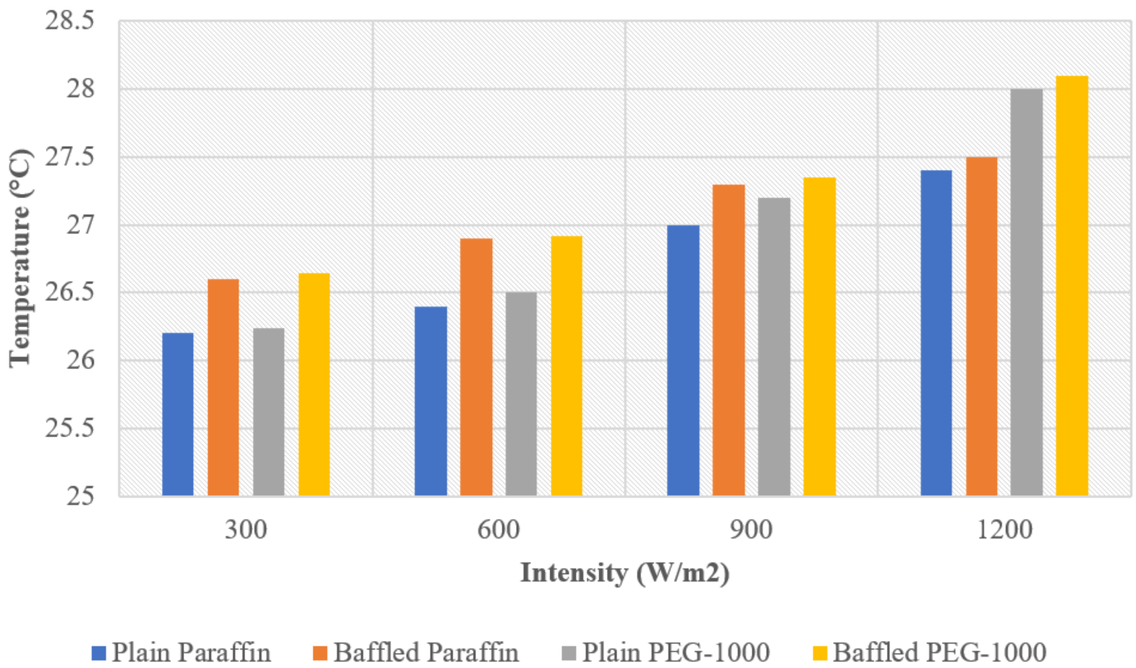

Figure 6. Comparison of the thermal PV cell

Figure 7 compares the PV cell efficiency after integrating paraffin- and PEG-1000-based PCMs with plain and baffled container designs at different radiation intensity levels. In general, efficiency increases as intensity increases, but the rate of improvement varies between configurations. At an intensity of 300 W/m², the highest efficiency was obtained using plain paraffin at 5.3%, while the baffled paraffin configuration recorded the lowest efficiency at 5.1%. As the intensity increased to 1200 W/m², the highest efficiency value was still achieved by plain paraffin at 11.7%, while baffled PEG-1000 showed a highly competitive value of 11.18%. This indicates that the plain model is more effective in maintaining PV cell temperature stability and efficiency performance in high radiation conditions. The performance advantages of plain paraffin are closely related to the thermal characteristics of paraffin, which has a high latent heat capacity, a melting point suitable for tropical conditions, and a more stable latent energy release rate compared to PEG-1000. This absorption-based cooling mechanism and latent heat discharge significantly reduce PV cell temperature fluctuations, thus maintaining more consistent electrical performance in the long run.

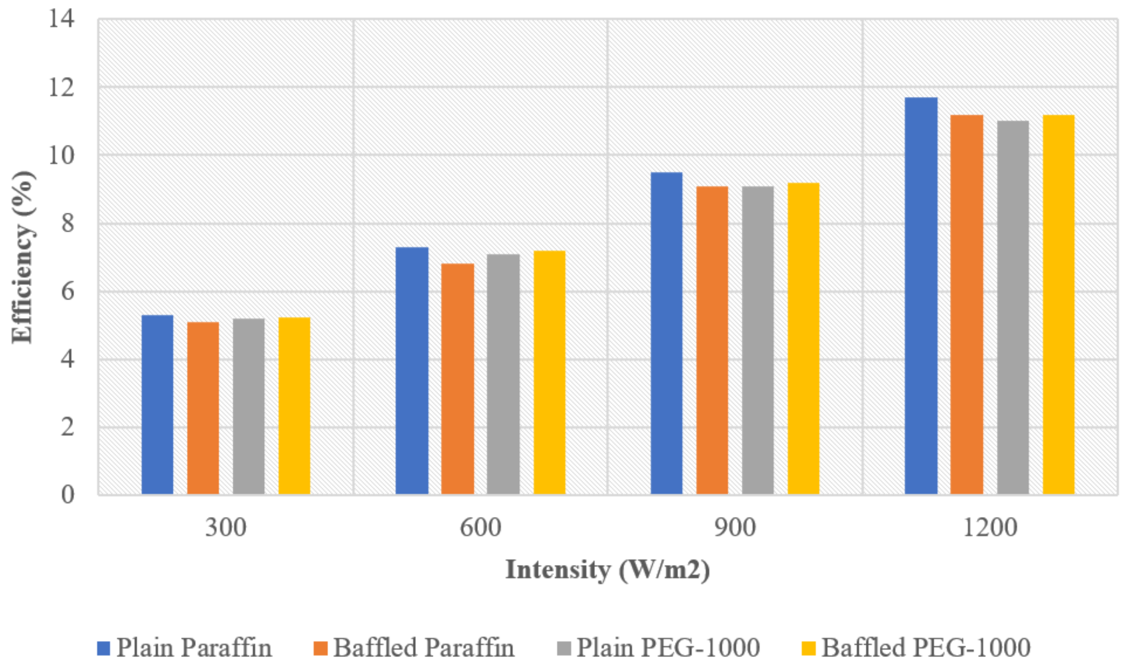

Figure 7. Comparison of the PV cell efficiency

The observed differences in system performance across the container configurations can be attributed to the fundamental heat transfer mechanisms influenced by geometry. In baffled containers, the internal partitions create a more complex heat transfer pathway, increasing thermal resistance but potentially enhancing localized conduction and delaying complete PCM melting. This can stabilize the heat absorption process but may also lead to non-uniform thermal fields. On the other hand, plain containers allow more direct and rapid thermal propagation across the PCM volume, enabling a faster and more uniform phase change. This explains why the plain paraffin configuration, with its high latent heat and simpler geometry, consistently outperforms others in maintaining lower PV temperatures and higher efficiencies, particularly under high radiation conditions. Such performance aligns with Fourier's law, where simplified geometry promotes greater conductive flux across the PV-PCM interface, enhancing latent heat utilization efficiency.

The data presented in Figure 7 were cross-validated with the numerical outputs summarized in Table 3 to ensure consistency and traceability. Every efficiency data point in the figure corresponds directly to the recorded peak operating temperature and computed efficiency using Eq. (6). For instance, the 11.7% efficiency value for plain paraffin at 1200 W/m² directly correlates with its thermal profile and minimum PV temperature of 27.4°C. Similarly, the 11.18% efficiency of baffled PEG-1000 is supported by its corresponding temperature range and PCM melting fraction during the transient simulation. This verification ensures that visual representations align precisely with simulation outputs and maintain scientific accuracy.

5 Conclusions

This study focuses on numerical analysis of the performance of the PVT system integrated with PCM based on paraffin and PEG-1000 using two different container designs, namely plain container and baffled container. Numerical simulations based on CFD were performed to evaluate PV cells' temperature distribution and efficiency under variations in solar radiation intensity between 300 and 1200 W/m². The simulation results showed that all PCM configurations could significantly reduce the operating temperature of the PV cell compared to conditions without PCM. Plain container models, especially with paraffin materials, proved more effective in maintaining low temperature stability and the system's thermal efficiency than baffled models. At an intensity of 1200 W/m², plain paraffin maintained the PV cell temperature at 27.4°C with the highest efficiency of 11.7%. The baffle structure did improve internal heat distribution. Still, in some cases, it accelerated the accumulation of local heat, which impacted the increase in the average temperature of the PV cell. The advantages of paraffin lie in its high latent heat capacity, phase stability, and thermal response speed corresponding to the dynamics of daily heat loads. Therefore, for PVT-PCM applications in hot climates, using paraffin with a plain container design is recommended as an optimal solution to improve energy efficiency, extend the system's operational life, and support sustainable solar energy technology.

Beyond summarizing the simulation results, this study provides practical insights into designing and optimizing passive thermal regulation for PV modules using PCM. The outcomes contribute to the broader goal of enhancing the reliability and efficiency of solar energy systems in hot climates. Future studies are encouraged to validate these findings experimentally, investigate long-term material stability under real environmental conditions, and explore advanced PCM composites such as those enhanced with nanoparticles or embedded fins to improve heat transfer performance further. Additionally, integrating intelligent thermal management systems could unlock adaptive cooling strategies, offering new directions for research in innovative, energy-efficient solar technologies.

Data Availability

The data used to support the findings of this study are available from the corresponding author upon request.

Acknowledgements

This paper is the result of research entitled “Pengembangan Konfigurasi Geometri Heatsinkphase Changes Material Untuk Meningkatkan Efisiensi Listrik Sel Surya Fotovoltaik," funded by the State University of Malang through the Penelitian Pemula scheme with contract No.: 24.2.283/UN32.14.1/LT/2025. The entire research and manuscript are under the guidance and chairmanship of Dr. Singgih Dwi Prasetyo, affiliated with Power Plant Engineering Technology, State University of Malang, Malang 65145, Indonesia.

Conflicts of Interest

The authors declare no conflict of interest.

References

[1] K. S. Kumar, S. Revanth, D. Sanjeev, P. S. Kumar, and P. Surya, “Experimental investigation of improving the energy conversion efficiency of PV cell by integrating with PCM,” *Mater. Today Proc.*, vol. 37, no. 2, pp. 712–716, 2020. https://doi.org/10.1016/j.matpr.2020.05.723

[2] S. Fan, X. Wang, S. Cao, Y. Wang, Y. Zhang, and B. Liu, “A novel model to determine the relationship between dust concentration and energy conversion efficiency of photovoltaic (PV) panels,” *Energy*, vol. 252, p. 123927, 2022. https://doi.org/10.1016/j.energy.2022.123927

[3] Z. Arifin, S. D. Prasetyo, T. Triyono, C. Harsito, and E. Yuniastuti, “Rancang bangun mesin pencacah limbah kotoran sapi,” *J. Rekayasa Mesin*, vol. 11, no. 2, pp. 187–197, 2020.

[4] A. Shafiei Ghazani, H. Nasiraei, M. Najafzadeh, and A. Fathollahzadehsardroudi, “Thermal management of photovoltaic panel by honeycomb-like metal structure filled with phase change material,” *Int. Commun. Heat Mass Transf.*, vol. 156, p. 107649, 2024. https://doi.org/10.1016/j.icheatmasstransfer.2024.107649

[5] J. Paul, A. K. Pandey, Y. N. Mishra, Z. Said, Y. K. Mishra, Z. Ma, J. Jacob, K. Kadirgama, M. Samykano, and V. V. Tyagi, “Nano-enhanced organic form stable pcms for medium temperature solar thermal energy harvesting: Recent progresses, challenges, and opportunities,” *Renew. Sustain. Energy Rev.*, vol. 161, p. 112321, 2022. https://doi.org/10.1016/j.rser.2022.112321

[6] Z. Arifin, S. Hadi, H. N. Jati, S. D. Prasetyo, and Suyitno, “Effect of electrospinning distance to fabricate Zno nanofiber as photoanode of dye-sensitized solar cells,” *AIP Conf. Proc.*, vol. 2217, p. 030095, 2020. https://doi.org/10.1063/5.0000705

[7] X. Wang, W. Li, Z. Luo, K. Wang, and S. P. Shah, “A critical review on phase change materials (PCM) for sustainable and energy efficient building: Design, characteristic, performance and application,” *Energy Build.*, vol. 260, p. 111923, 2022. https://doi.org/10.1016/j.enbuild.2022.111923

[8] A. NematpourKeshteli, M. Iasiello, G. Langella, and N. Bianco, “Using metal foam and nanoparticle additives with different fin shapes for PCM-based thermal storage in flat plate solar collectors,” *Therm. Sci. Eng. Prog.*, vol. 52, p. 102690, 2024. https://doi.org/10.1016/j.tsep.2024.102690

[9] V. K. Sonker, P. Sharma, R. Ram, and A. Sarkar, “A CFD simulation analysis of the effects of PCM and nanoparticles stored in copper cylinders inside a solar still,” *J. Energy Storage*, vol. 108, p. 115091, 2024. https://doi.org/10.1016/j.est.2024.115091

[10] R. Bhandari and J. K. Devanuri, “Effect of duct geometry on thermal management of PCM – liquid hybrid PV panel,” *J. Phys. Conf. Ser.*, vol. 2178, no. 012008, 2020. https://doi.org/10.1088/1742-6596/2178/1/012008

[11] Z. Arifin, S. D. Prasetyo, B. A. Tribhuwana, D. D. D. P. Tjahjana, R. A. Rachmanto, and B. Kristiawan, “Photovoltaic performance improvement with phase change material cooling treatment,” *Int. J. Heat Technol.*, vol. 40, no. 4, pp. 953–960, 2022. https://doi.org/10.18280/ijht.400412

[12] Y. Trisnoaji, S. D. Prasetyo, M. S. Mauludin, C. Harsito, and A. Anggit, “Computational fluid dynamics evaluation of nitrogen and hydrogen for enhanced air conditioning efficiency,” *J. Ind. Intell.*, vol. 2, no. 3, pp. 144–159, 2024. https://doi.org/10.56578/jii020302

[13] A. Khanlari, I. Aytac, A. D. Tuncer, H. I. Variyenli, and H. N. Sahin, “Improving the performance of a PCM integrated solar air collector by adding porous fins over the bottom side of the absorber: A transient CFD study,” *J. Energy Storage*, vol. 90, p. 111847, 2024. https://doi.org/10.1016/j.est.2024.111847

[14] Y. Khattari, A. Arid, A. El Ouali, T. Kousksou, I. Janajreh, and E. M. B. Ghoulam, “CFD study on the validity of using PCM in a controlled cooling ceiling integrated in a ventilated room,” *Dev. Built Environ.*, vol. 9, p. 100066, 2022. https://doi.org/10.1016/j.dibe.2021.100066

[15] A. Salari, A. Kazemian, T. Ma, A. Hakkaki-Fard, and J. Peng, “Nanofluid based photovoltaic thermal systems integrated with phase change materials: Numerical simulation and thermodynamic analysis,” *Energy Convers. Manag.*, vol. 205, p. 112384, 2020. https://doi.org/10.1016/j.enconman.2019.112384

[16] M. A. Sheik, M. K. Aravindan, N. Beemkumar, P. K. Chaurasiya, and J. A. Dhanraj, “Enhancement of heat transfer in PEG 1000 using nano-phase change material for thermal energy storage,” *Arab. J. Sci. Eng.*, vol. 47, no. 12, pp. 15 899–15 913, 2022. https://doi.org/10.1007/s13369-022-06810-9

[17] M. A. Ali, Fayaz, R. F. Viegas, M. B. Shyam Kumar, R. K. Kannapiran, and M. Feroskhan, “Enhancement of heat transfer in paraffin wax PCM using nano graphene composite for industrial helmets,” *J. Energy Storage*, vol. 26, p. 100982, 2019. https://doi.org/10.1016/j.est.2019.100982

[18] A. Shahsavar, A. H. A. Alwaeli, N. Azimi, S. Rostami, K. Sopian, M. Arıcı, P. Estellé, S. Nižetić, A. Kasaeian, H. M. Ali, Z. Ma, and M. Afrand, “Exergy studies in water-based and nanofluid-based photovoltaic/thermal collectors: Status and prospects,” *Renew. Sustain. Energy Rev.*, vol. 168, p. 112740, 2022. https://doi.org/10.1016/j.rser.2022.112740

[19] H. Ebrahimi, H. S. Akhijahani, and P. Salami, “Improving the thermal efficiency of a solar dryer using phase change materials at different position in the collector,” *Sol. Energy*, vol. 220, pp. 535–551, 2021. https://doi.org/10.1016/j.solener.2021.03.054

[20] S. Aneli, R. Arena, and A. Gagliano, “Numerical simulations of a PV module with phase change material (PV-PCM) under variable weather conditions,” *Int. J. Heat Technol.*, vol. 39, no. 2, pp. 643–652, 2021. https://doi.org/10.18280/ijht.390236

[21] A. Chibani, S. Merouani, H. Laidoudi, A. Dehane, L. Bendada, L. Lamiri, G. Mecheri, C. Bougriou, and N. Gherraf, “Numerical simulation and analysis of heat transfer and melting rate of nano-enhanced PCM composite embedded in a concentrator photovoltaic system,” *J. Energy Storage*, vol. 73, p. 109247, 2023. https://doi.org/10.1016/j.est.2023.109247

[22] E. J. Mahdi, S. Algburi, N. Al-Abadi, O. K. Ahmed, and A. K. Ahmed, “Photovoltaic panel cooling using ground source energy: CFD simulation,” *Results Eng.*, vol. 22, p. 102144, 2024. https://doi.org/10.1016/j.rineng.2024.102144

[23] H. A. Maarof, V. M. Avargani, I. E. Maree, and A. H. Yaseen, “CFD modeling of a tubular three-pass solar air heater with phase change material: Investigating heat transfer enhancement and energy efficiency,” *J. Energy Storage*, vol. 87, p. 111522, 2024. https://doi.org/10.1016/j.est.2024.111522

[24] D. Guerraiche, C. Bougriou, K. Guerraiche, L. Valenzuela, and Z. Driss, “Experimental and numerical study of a solar collector using phase change material as heat storage,” *J. Energy Storage*, vol. 27, p. 101133, 2020. https://doi.org/10.1016/j.est.2019.101133

[25] J. M. Mahdi, H. M. T. Al-Najjar, H. Togun, N. Biswas, M. Boujelbene, S. Alshammari, and P. Talebizadehsardari, “Year-round performance evaluation of photovoltaic-thermal collector with nano-modified phase-change material for building application in an arid desert climate zone,” *Energy Build.*, vol. 320, p. 114597, 2024. https://doi.org/10.1016/j.enbuild.2024.114597

[26] S. Manikandan, G. Muthuvairavan, M. Samykano, and S. K. Natarajan, “Numerical simulation of various PCM container configurations for solar dryer application,” *J. Energy Storage*, vol. 86, p. 111294, 2024. https://doi.org/10.1016/j.est.2024.111294

[27] M. Khodadadi and M. Sheikholeslami, “Assessment of photovoltaic thermal unit equipped with phase change material in different finned containers,” *J. Energy Storage*, vol. 46, p. 103939, 2022. https://doi.org/10.1016/j.est.2021.103939

[28] E. H. Amalu and O. A. Fabunmi, “Thermal control of crystalline silicon photovoltaic (c-Si PV) module using docosane phase change material (PCM) for improved performance,” *Sol. Energy*, vol. 234, pp. 203–221, 2022. https://doi.org/10.1016/j.solener.2022.02.001

[29] N. B. S. Selabi, A. R. K. Lenwoue, and L. D. W. Djouonkep, “Numerical investigation of the optimization of PV-system performances using a composite PCM-metal matrix for PV-solar panel cooling system,” *J. Fluid Flow Heat Mass Transf.*, vol. 8, pp. 262–274, 2021. https://doi.org/10.11159/jffhmt.2021.028

[30] Z. Fan, Y. Zhao, X. Liu, Y. Shi, and D. Jiang, “Thermal properties and reliabilities of lauric acid-based binary eutectic fatty acid as a phase change material for building energy conservation,” *ACS Omega*, vol. 7, no. 18, pp. 16 097–16 108, 2022. https://doi.org/10.1021/acsomega.2c01420

[31] M. Jurčević, S. Nižetić, I. Marinić-Kragić, M. Jakić, and M. Arıcı, “Towards resilient operation of photovoltaic-thermal collector with incorporated organic phase change material: Numerical and experimental investigation,” *Sustain. Energy Technol. Assess.*, vol. 60, p. 103465, 2023. https://doi.org/10.1016/j.seta.2023.103465

[32] H. Shakibi, A. Shokri, B. Sobhani, and M. Yari, “Numerical analysis and optimization of a novel photovoltaic thermal solar unit improved by nano-PCM as an energy storage media and finned collector,” *Renew. Sustain. Energy Rev.*, vol. 179, p. 113230, 2023. https://doi.org/10.1016/j.rser.2023.113230

[33] Z. Arifin, S. D. Prasetyo, Y. J. Prasojo, D. D. D. P. Tjahjana, R. A. Rachmanto, A. R. Prabowo, and A. Larasati, “Computational fluid dynamics investigation: The effect of phase change material addition on thermal collector system performance,” *AIP Conf. Proc.*, vol. 3124, no. 1, 2024. https://doi.org/10.1063/5.0227754

[34] N. Azimi, E. Sharifzadeh, M. Rahimi, and M. Nouira, “Improving the performance of photovoltaic panels integrated with ultrasound and phase change materials: Experimental study and CFD modeling,” *J. Therm. Anal. Calorim.*, vol. 149, no. 15, pp. 8193–8213, 2024. https://doi.org/10.1007/s10973-024-13295-1

[35] S. D. Prasetyo, A. R. Prabowo, and Z. Arifin, “The use of a hybrid photovoltaic/thermal (PV/T) collector system as a sustainable energy-harvest instrument in urban technology,” *Heliyon*, vol. 9, no. 2, p. e13390, 2023. https://doi.org/10.1016/j.heliyon.2023.e13390